Published in final edited form as:
Clin Cancer Res. 2014 June 1; 20(11): 2947–2958. doi:10.1158/1078-0432.CCR-13-3448.

Ganitumab (AMG 479) Inhibits IGF-II–Dependent Ovarian Cancer Growth and Potentiates Platinum-Based Chemotherapy

Pedro J. Beltran[1], **Frank J. Calzone**[1], **Petia Mitchell**[1], **Young-Ah Chung**[1], **Elaina Cajulis**[1], **Gordon Moody**[1], **Brian Belmontes**[1], **Chi-Ming Li**[2], **Steven Vonderfecht**[3], **Victor E. Velculescu**[5], **Guorong Yang**[4], **Jingwei Qi**[4], **Dennis J. Slamon**[4], and **Gottfried E. Konecny**[4]

[1]Oncology Research Therapeutic Area, Amgen Inc., Thousand Oaks [2]Genomics Analysis Unit, Amgen Inc., Thousand Oaks [3]Department of Pathology, Amgen Inc., Thousand Oaks [4]Division of Hematology-Oncology, Department of Medicine, David Geffen School of Medicine, University of California Los Angeles, Los Angeles, California [5]The Ludwig Center and the Howard Hughes Medical Institute, Kimmel Cancer Center, Johns Hopkins Medical Institutions, Baltimore, Maryland

Abstract

Purpose—Insulin-like growth factor 1 receptor (IGF-IR) has been implicated in the pathogenesis of ovarian cancer. Ganitumab is an investigational, fully human monoclonal antibody against IGF-IR. Here, we explore the therapeutic potential of ganitumab for the treatment of ovarian cancer.

Experimental Design—The effects of ganitumab were tested *in vitro* against a panel of 23 established ovarian cancer cell lines. The ability of ganitumab to inhibit IGF-I–, IGF-II–, and insulin-mediated signaling was examined *in vitro* and in tumor xenografts using ovarian cancer models displaying IGF-IR/PI3K/AKT pathway activation by two distinct mechanisms, PTEN loss

Corresponding Author: Pedro J. Beltran, Amgen Inc., One Amgen Center Drive, Thousand Oaks, CA 91320. Phone: 805-447-9221; Fax: 805-375-8524; pbeltran@amgen.com.
P. Mitchell, Y.-A. Chung, G. Moody, B. Belmontes, and E. Cajulis contributed equally to this article, and author order was randomly determined.

Note: Supplementary data for this article are available at Clinical Cancer Research Online (http://clincancerres.aacrjournals.org/).

Disclosure of Potential Conflicts of Interest
F.J. Calzone has ownership interest (including patents) in and is a consultant/advisory board member for Amgen. C.-M. Li is an employee of and reports receiving a commercial research grant from Amgen. V.E. Velculescu has ownership interest in a patent regarding PIK3CA in human cancer. No potential conflicts of interest were disclosed by the other authors.

Authors' Contributions
Conception and design: P.J. Beltran, F.J. Calzone, G. Moody, C.-M. Li, D.J. Slamon, G.E. Konecny
Development of methodology: P.J. Beltran, G. Moody, C.-M. Li, V.E. Velculescu, J. Qi, D.J. Slamon, G.E. Konecny
Acquisition of data (provided animals, acquired and managed patients, provided facilities, etc.): P. Mitchell, Y.-A. Chung, E. Cajulis, G. Moody, B. Belmontes, C.-M. Li, S. Vonderfecht, V.E. Velculescu, G. Yang, J. Qi, G.E. Konecny
Analysis and interpretation of data (e.g., statistical analysis, biostatistics, computational analysis): P.J. Beltran, F.J. Calzone, P. Mitchell, Y.-A. Chung, G. Moody, B. Belmontes, C.-M. Li, S. Vonderfecht, V.E. Velculescu, J. Qi, G.E. Konecny
Writing, review, and or revision of the manuscript: P.J. Beltran, G. Moody, C.-M. Li, S. Vonderfecht, G.E. Konecny
Administrative, technical, or material support (i.e., reporting or organizing data, constructing databases): P.J. Beltran, P. Mitchell, E. Cajulis, J. Qi, D.J. Slamon, G.E. Konecny
Study supervision: P.J. Beltran, G. Moody, V.E. Velculescu, G.E. Konecny

and IGF-II overexpression. Drug interactions between ganitumab and cisplatin, carboplatin, or paclitaxel were studied *in vitro* and *in vivo*.

Results—*In vitro*, growth inhibition varied significantly among individual ovarian cancer cell lines. IGF-II mRNA and phospho–IGF-IR protein expression were quantitatively correlated with response to ganitumab, and PTEN mutations conferred resistance to ganitumab. Ganitumab potently inhibited baseline and IGF-I–, IGF-II–, and insulin-induced IGF-IR and IGF-IR/insulin hybrid receptor signaling *in vitro* and *in vivo*. Synergistic and additive drug interactions were seen for ganitumab and carboplatin or paclitaxel *in vitro*. Furthermore, ganitumab significantly increased the efficacy of cisplatin in ovarian cancer xenograft models *in vivo*.

Conclusions—These observations provide a biologic rationale to test ganitumab as a single agent or in combination with carboplatin/cisplatin and paclitaxel in patients with ovarian cancer. Moreover, assessment of tumor expression of IGF-II, phospho–IGF-IR, or PTEN status may help select patients with ovarian cancer who are most likely to benefit from ganitumab.

Introduction

Ovarian cancer is the leading cause of death from gynecologic malignancies in the developed world (1). Despite radical surgery and initial high response rates to platinum-and taxane-based chemotherapy, almost all ovarian cancer recurs at a median of 18 to 24 months from diagnosis (2, 3). Advances in the understanding of the molecular pathogenesis of ovarian cancer coupled with the development of novel, targeted therapies are needed to improve patient outcomes. Alterations of the insulin-like growth factor 1 receptor (IGF-IR) signaling axis are a common molecular finding in ovarian cancer and may be of potential therapeutic utility (4).

The IGF-IR signaling axis is composed of 2 receptors, IGF-IR and the insulin receptor (INSR); 3 ligands, IGF-I, IGF-II, and insulin; and 6 binding proteins that are believed to be important regulators of IGF signaling by determining bio-availability of IGF-I and IGF-II (5). Adding further complexity, 2 distinct splice variants of INSR (INSRA, INSRB) and IGF-IR exist that can form various homo- and heterodimers (6–8).

In vitro and *in vivo* studies have shown that IGFIR, IGF-I, IGF-II, and IGF-binding proteins are key regulators of ovarian follicular growth, selection, and cellular differentiation (9, 10). Moreover, IGF-IR is expressed in most human ovarian cancers (11, 12). The strongest link between the IGF-IR signaling axis and ovarian cancer comes from IGF-II. High levels of IGF-II have been associated with disease progression and poor survival in patients with ovarian cancer (13, 14). Recent genome-wide association studies have shown that genetic variations of the IGF-II gene are associated with an increased risk of developing epithelial ovarian cancer (15). IGF-II expression is subject to genomic imprinting, leading to transcription from only the paternal allele. Loss of imprinting from relaxed control of the maternal allele leads to increased expression of IGF-II in multiple tumor types, including ovarian cancer (16, 17). Recent preclinical studies indicate that IGF-II can modulate resistance of ovarian cancer cells to chemotherapeutic agents such as paclitaxel (18). Together, these studies suggest that inhibition of the IGF/IGF-IR signaling pathway may be a promising approach for the treatment of patients with ovarian cancer.

Ganitumab is an investigational, fully human monoclonal antibody (IgG1) against IGF-IR that inhibits the binding of IGF-IR and hybrid receptors to their endogenous ligands IGF-I (IC_{50}: 0.5 nmol/L) and IGF-II (IC_{50}: 0.6 nmol/L; ref. 19). Here, we evaluate ganitumab as a potential therapeutic agent for the treatment of ovarian cancer, either alone or in combination with chemotherapy. We first tested the *in vitro* effects of ganitumab against a panel of 23 ovarian cancer cell lines, representing all histologic subtypes of the disease. Molecular markers for response prediction, including IGF-II expression, IGF-IR phosphorylation, and PTEN mutations, were studied using gene expression profiling, mesoscale discovery (MSD) assays, and sequencing. To more fully understand the antiproliferative effects, we studied the ability of ganitumab to inhibit IGF-I–, IGF-II–, and insulin-mediated signaling of IGF-IR homodimers and IGF-IR/INSR hybrids in ovarian cancer models displaying IGF-IR/PI3K/AKT pathway activation by 2 distinct mechanisms PTEN loss and IGF-II overexpression. Drug interactions between ganitumab and chemotherapeutic agents commonly used for the treatment of ovarian cancer were studied using *in vitro* and *in vivo* experiments. Our findings suggest that ganitumab could offer benefit in combination with platinum agents and paclitaxel in a biomarker-selected group of ovarian carcinomas.

Materials and Methods

Cell lines and reagents

The effects of ganitumab on growth inhibition were studied in a panel of 23 established human ovarian cancer cell lines. Individuality of each cell line was checked by mitochondrial DNA sequencing. Cell lines were passaged for fewer than 3 months after authentication. Additional information on the cell lines is provided in Supplementary Table S1. Platinum analogs carboplatin and cisplatin were obtained from Bristol-Myers Squibb and PCH Pharmachemie, respectively. Paclitaxel was obtained from Mead Johnson/Bristol-Myers Squibb. IGF-I, IGF-II, and insulin were obtained from Sigma.

Growth inhibition assays

Anchorage-dependent growth was assessed by plating ovarian cancer cell lines into 24-well tissue culture plates at a density of 2×10^5 to 5×10^5 and growing the cells with or without 100 μg/mL (0.68 μmol/L) ganitumab. Cells were harvested by trypsinization on day 7 and counted using a particle counter (Z1, Beckman Coulter Inc.). Experiments were performed at least 3 times in duplicate for each cell line.

Additional experiments were performed with OV-90 and TOV-21G cells seeded in 96-well plates in complete media with either 0.5 μmol/L ganitumab or human IgG1 (hIgG1). Confluence measurements were performed in duplicate for each well at 4-hour intervals over 5 to 7 days using an IncuCyte phase contrast optical imaging system (Essen Instruments).

To study the inhibition of anchorage-independent growth, soft agar assays were performed. A 0.5% agar solution (Difco Agar Noble, BD) was placed on the bottom of a 24-well plate. Cells were seeded in quadruplicates at a density of 5×10^3 and mixed into a 0.3% agar top

layer that had been prepared with or without 100 μg/mL (0.68 μmol/L) ganitumab. Culture plates were stored at 37°C, 5% CO_2 for up to 5 weeks. Colonies were stained with Neutral Red solution (Sigma-Aldrich) and counted by visual inspection. All assays were performed at least 3 times in duplicate for each cell line.

Gene expression profiling

Microarray hybridizations have been previously performed in the 23 ovarian cell lines at baseline using the Agilent Human 44 K array chip. The techniques used have been described in detail elsewhere (20). The original data are available online with the GEO accession number GSE26805.

Mutational analysis of PIK3CA, PIK3R1, KRAS, BRAF, and PTEN

The coding regions of the *PIK3CA, PIK3R1, KRAS, BRAF*, and *PTEN* genes in each cell line were sequenced using next-generation sequencing (Personal Genome Diagnostics, Inc.). and assessed for potential sequence alterations using approaches previously described (21).

TaqMan analysis of *INSRA, INSRB, IGF-IR*, and *IGF-II* expression

DNaseI-treated total RNA (20–40 ng) was used for the quantitative reverse transcription PCR (qRT-PCR) assays by following the commercial instructions. In brief, the combination of the primers and the TaqMan probe for each assay was added to the 1× ABI TaqMan one-step RT-PCR master mix reagents containing RT mix (ABI/Life Technologies) at the ratio of 2:1 (400:200 nmol/L). After 25 to 30 minutes of reverse transcription reaction at 50°C, quantitative PCR was performed by running the program of heat activation of Taq DNA polymerase at 95°C for 10 minutes followed by 40 cycles at 95°C for 10 seconds and 60°C for 1 minute in ABI 7900 SDS system (ABI/Life Technologies). After normalization and data analysis, the expression of the examined genes was determined relative to the expression of the control gene *HPRT1*. Primer sets are shown in Supplementary Table S2.

Western blotting for PTEN and AKT

OV-90 and TOV-21G cells were cultured in 100-mm dishes in complete media. At 80% confluence, cells were washed with cold PBS and lysed in 300 μL of radio-immunoprecipitaion assay (RIPA) lysis buffer. The lysates were cleared by centrifugation, and 10 μg of total protein was applied to a NuPage 4% to 12% Bis-Tris electrophoresis gel. Total protein level was detected after transfer to a polyvinylidene difluoride membrane using the following antibodies: (i) Cell Signaling Technologies #9552 for PTEN, (ii) Biosource #44–621G for phospho-AKT, (iii) Cell Signaling Technologies #9272 for total AKT, and (iv) Sigma #T7816 for β-tubulin. Primary antibody signal was detected with horseradish peroxidase–conjugated secondary antibodies using Super Signal West Pico detection reagent (Pierce Bio). Quantification was performed using a VersaDoc instrument and Quantity One Software (Bio-Rad).

Flow cytometry for IGF-IR and INSR

OV-90 and TOV-21G cells were harvested and incubated with 1 μg phycoerythrin (PE)-conjugated anti-human IGF-IR or anti-human INSR monoclonal antibodies (BD

Pharmingen) at 4°C for 1.5 hours. Mean fluorescence levels were determined by flow cytometry and converted to absolute levels of IGF-IR and INSR using Quantum microbeads (Bangs Laboratories).

Multiplex ELISA assays

The levels of total and phosphorylated IGF-IR, INSR, IRS-1, AKT, S6 kinase, and GSK3β protein expression were studied using MSD assays. To determine the effect of ganitumab on baseline signaling of IGF-IR, INSR, and their downstream signaling intermediates in the ovarian cancer cell line panel, cell lines were plated in 6-well tissue culture dishes and cultured for 24 hours under standard conditions before treatment with 100 μg/mL (0.68 μmol/L) ganitumab for 1 hour. To determine the effect of ganitumab on ligand-induced activation of IGF-IR, INSR, and AKT, OV-90 and TOV-21G cells were serum-starved for 24 hours and incubated with IGF-I, IGF-II (Sigma), or insulin (0–200 nmol/L, Amgen Inc.) for 20 minutes. The experiments were repeated with fixed concentrations of ligands plus a range of ganitumab concentrations (0–1 μmol/L). Cells were lysed in MSD complete lysis buffer. Following centrifugation, the supernatant was collected, and the protein concentration was determined using a bicinchoninic acid (BCA) assay, following the manufacturer's instructions. Ten micrograms of protein was added to the plate in duplicate wells and incubated overnight at 4°C MSD 96-well multispot assays were carried out per the manufacturer's protocol, which has been described in detail elsewhere (22).

Multiple drug effect analysis

Multiple drug effect analysis using ganitumab in combination with carboplatin and paclitaxel was performed as described previously (23). Combination index values were derived from variables of the median effect plots, and statistical tests were applied to determine whether the mean combination index values at multiple effect levels (IC_{20}–IC_{80}) were significantly different from 1.0. In this analysis, synergy was defined as combination index values significantly lower than 1.0, antagonism was defined as combination index values significantly higher than 1.0, and additivity as combination index values equal to 1.0.

In vivo pharmacodynamic studies

Female, 4- to 6-week-old, athymic nude mice (Harlan Sprague Dawley Labs) were used in all experiments. The laboratory housing the cages had a 12-hour light/dark cycle and met all AAALAC specifications. All experimental procedures were performed in accordance with IACUC and USDA regulations. Water and food were supplied *ad libitum*. OV-90 or TOV-21G cells were injected subcutaneously (5 million per mouse). When the average tumor size reached approximately 300 to 450 mm^3, mice were randomly assigned into 4 groups (3 mice per group). Two groups of mice were pretreated with 1 μg ganitumab and 2 with 1 μg hIgG1 by intraperitoneal injection. After 6 hours, one ganitumab and one hIgG1 group received human IGF-I (15 μg) by intravenous injection. Control groups received 1× PBS. Xenografts were collected 15 minutes after IGF-I challenge and snap frozen in liquid nitrogen. Samples were homogenized and prepared as previously described (19).

Detection of bromodeoxyuridine in ganitumab-treated xenografts

Bromodeoxyuridine (BrdUrd) detection in xenografts was performed as previously described (24). Briefly, incorporation of BrdUrd in tumor sections was detected with a rat anti-BrdU antibody (Accurate), a biotin-labeled rabbit anti-rat IgG secondary antibody (Vector Laboratories), and Vectastain Elite ABC detection kit (Vector Laboratories).

Xenograft efficacy studies

Female *nu/nu* CD1 mice bearing established (~200 mm^3) OV-90 or TOV-21G xenografts were randomly assigned into 4 groups (10 mice per group) and treated intraperitoneally twice per week with ganitumab (30, 100, or 300 μg/dose), hIgG1 (300 μg/dose), cisplatin (2.5 or 4.0 mg/kg), or ganitumab plus cisplatin for the duration of the experiment. Tumor volumes and body weights were measured twice per week using calipers and an analytical scale, respectively.

Statistical analysis

Ganitumab dose–response experiments were analyzed by repeated-measures ANOVA (RMANOVA) followed by the *post hoc* Scheffe test to compare reduction in tumor volume in the ganitumab-treated groups versus the hIgG1 group. Combination studies using ganitumab and cisplatin were analyzed using RMANOVA to compare the combination with each agent alone. Changes in phospho–IGF-IR phos-pho-INSR, and phospho-AKT in the pharmacodynamic assay were compared using the Student *t* test. Associations between biomarkers and *in vitro* sensitivity (% growth inhibition) were analyzed using Spearman rho correlation.

Results

Growth inhibition of ovarian cancer cell lines *in vitro*

The effects of ganitumab on human ovarian cancer cells were initially evaluated using a panel of 23 established human ovarian cancer cell lines (Supplementary Table S1). These cell lines were selected to be representative of a range of ovarian cancer subtypes. Anchorage-dependent growth inhibition varied significantly between individual cell lines when treated with 100 μg/mL (0.68 μmol/L) ganitumab and ranged between 45% in KK cells to no significant growth inhibition in COLO704 (Fig. 1A).

Next, we studied the effect of ganitumab on anchorage-independent growth using soft agar assays. Of the 23 tested cell lines, 16 ovarian cancer cell lines formed colonies in soft agar (Supplementary Table S1). Again, the inhibition of colony formation varied significantly between individual cell lines when treated with 100 μg/mL (0.68 μmol/L) ganitumab and ranged between 90% in sensitive cell lines such as OV-90 or OVCAR-3 to no-growth inhibition in resistant cell lines such as COLO704 (Fig. 1B).

There was no statistically significant correlation between the histologic subtype of the cell lines and sensitivity to ganitumab (data not shown). However, following molecular characterization of the IGF/IGF-IR signaling pathway in each of the 23 ovarian cancer cell lines using gene expression profiling, multiplex ELISA assays, and sequencing of *PIK3CA*,

PI3KR1, *PTEN*, *KRAS*, and *BRAF*, we were able to show that either anchorage-dependent or anchorage-independent growth inhibition by ganitumab was correlated with increased expression of phospho–IGF-IR ($r = 0.47$, $P = 0.024$ and $r = 0.67$, $P = 0.005$, respectively) and its ligand IGF-II ($r = 0.33$, $P = 0.122$ and $r = 0.65$, $P = 0.006$, respectively). Conversely, the presence of PTEN mutations conferred resistance to ganitumab ($r = -0.57$, $P = 0.006$ and $r = -0.41$, $P = 0.118$, respectively; Fig. 1 and Supplementary Table S3).

Molecular characterization of ovarian cancer cell lines

To better understand the effects of ganitumab, 2 cell lines with opposite phenotypes were selected: OV-90 cells because they were responsive to ganitumab and TOV-21G because they were relatively unresponsive to ganitumab. Using quantitative flow cytometry, we first confirmed the number of cell-surface IGF-IRs and INSRs on OV-90 cells to be 30,500 per cell and 1,600 per cell, respectively. In comparison, TOV-21G cells expressed only 1,600 IGF-IRs per cell and 900 INSRs per cell on the cell surface (Supplementary Table S4). Analysis of PTEN and phospho-AKT expression by Western immunoblotting confirmed that TOV-21G cells were PTEN-null and displayed increased basal phospho-AKT expression levels relative to PTEN wild-type (WT) cell lines. In comparison, OV-90 cells expressed robust levels of PTEN expression and an undetectable level of pAKT in the absence of ligand stimulation (Supplementary Fig. S1).

Next we assessed IGF-II, IGF-IR, and INSRA expression in the OV-90 and TOV-21G cells and xenografts using TaqMan analyses. Expression of IGF-II in relationship to the housekeeping gene *HPRT1* was highest in OV-90 cells (88.6× in the cell line and 8.8× in the xenografts) and undetectable in TOV-21G cells, both of which are consistent with the gene expression data. Expression of IGF-IR in relationship to the housekeeping gene *HPRT1* was higher in OV-90 cells (3.0× in the cell line and 2.5× in the xenografts) when compared with TOV-21G cells (undetectable in the cell line and 0.2× in the xenografts). Finally, expression of INSRA in relationship to the housekeeping gene *HPRT1* was similar between OV-90 cells (0.4× in the cell line and 0.4× in the xenografts) and TOV-21G cells (undetectable in the cell line and 0.5× in the xenografts; Supplementary Table S4).

Time-dependent effect of ganitumab on viable cell numbers

The effect of ganitumab on viable cell numbers was determined in OV-90 and TOV-21G cells grown as adherent or nonadherent cultures in media containing 0%, 1%, or 10% serum. Growth curves (percentage of cell confluence) were generated to evaluate the time-dependent effect of ganitumab or hIgG1 on cell growth. Ganitumab treatment alone consistently increased the cell doubling time of OV-90 cells by 2-fold (Fig. 2A). In contrast, and consistent with the lack of effect of ganitumab on cell signaling in the TOV-21G cell line, ganitumab did not significantly affect the doubling time of TOV-21G cells (Fig. 2B). Interestingly, a slight tendency to a shorter doubling time was detected upon treatment of TOV-21G cells with ganitumab.

Effect of ganitumab on ligand-dependent activation of IGF-IR, INSR, and AKT

In OV-90 cells, IGF-I and insulin activated IGF-IR at low concentrations but did not display concentration-dependent activation. IGF-II, on the other hand, induced IGF-IR

phosphorylation in a concentration-dependent manner (Fig. 3A). Ganitumab potently inhibited basal and IGF-I–, IGF-II–, and insulin-induced IGF-IR phosphorylation in OV-90 cells.

Little to no change in IGF-IR phosphorylation was seen in TOV-21G cells following ligand stimulation with IGF-I, IGF-II, or insulin. TOV-21G cells were refractory to ganitumab inhibition of basal IGF-I–, IGF-II–, and insulin-induced IGF-IR phosphorylation (Fig. 3A).

In OV-90 and TOV-21G cells, all 3 ligands were able to induce potent INSR phosphorylation in a dose-dependent manner (Fig. 3B). The level of INSR phosphorylation in OV-90 cells was similar with each growth factor (INS, EC_{50} 4 nmol/L; IGF-I, EC_{50} 9 nmol/L; IGF-II, EC_{50} 18 nmol/L), whereas insulin was most potent in TOV-21G cells (INS, EC_{50} 4 nmol/L; IGF-I, EC_{50} 90 nmol/L; IGF-II, EC_{50} 53 nmol/L; Fig. 3B; Supplementary Table S5). In OV-90 cells, ganitumab inhibited IGF-I– and IGF-II–induced INSR phosphorylation back to basal level albeit at higher concentrations (IGF-I, EC_{50} 145 nmol/L; IGF-II, EC_{50} 155 nmol/L) than needed to inhibit IGF-IR (IGF-I, EC_{50} 6 nmol/L; IGF-II, EC_{50} 4.5 nmol/L). Ganitumab only minimally inhibited insulin-induced INSR phosphorylation in OV-90 cells (Fig. 3B). In the TOV-21G cell line, only IGF-I–induced INSR phosphorylation was partially inhibited by ganitumab. IGF-II– and insulin-driven signals were refractory to ganitumab (Fig. 3B).

The IGF-I– and IGF-II–induced phosphorylation of AKT in OV-90 cells paralleled that of activation of IGF-IR. However, the potency of ganitumab to inhibit AKT activation paralleled the inhibition of INSR phosphorylation (Fig. 3C), suggesting that most AKT activation was mediated through hybrid receptors. Insulin did not induce additional AKT activation in OV-90 cells, and ganitumab was not agonistic when used in the absence of growth factors. Ganitumab did not inhibit the high basal level of activated AKT detected in the TOV-21G cell line in the presence or absence of ligand (Fig. 3C).

Inhibition of IGF-I signaling in ovarian cancer xenografts

The contrasting effects of ganitumab on OV-90 and TOV-21G cells were further studied *in vivo* using a xenograft pharmacodynamic assay. In mice bearing OV-90 xenografts, administration of IGF-I (5 μg, intravenously) in the presence of control antibody (hIgG1) led to a 5-fold stimulation of IGF-IR and AKT phosphorylation (Fig. 4A). Pretreatment of mice with ganitumab led to a 50% inhibition of basal and 85% inhibition of IGF-I–induced IGF-IR activation. Ganitumab also led to a 50% inhibition of basal and 70% inhibition of IGF-I–induced AKT. Moreover, IGF-I also potently activated INSR expressed in OV-90 cells, and ganitumab was not able to inhibit this activation (Fig. 4A).

Mice bearing TOV-21G xenografts were insensitive to administration of IGF-I, showing no increase in IGF-IR, INSR, or AKT activation following injection of IGF-I. Treatment with ganitumab had no effect on basal or IGF-I– induced levels of phosphorylated IGF-IR, INSR, or AKT (Fig. 4B).

Growth inhibition of ovarian cancer xenograft models

Treatment of mice bearing established OV-90 xenografts with ganitumab significantly inhibited tumor growth in a dose-dependent manner. Ganitumab dosed at 30, 100, and 300 μg twice per week resulted in tumor growth inhibition of 42%, 100%, and 100%, respectively. Statistical significance ($P < 0.0001$) was reached in the 100 and 300 μg groups when compared with the hIgG1 group (Fig. 5A). Analysis of xenograft tissue remaining at the end of the study showed that ganitumab potently (>90%) inhibited IGF-IR activation at all 3 doses. Maximal inhibition was reached at the 100 μg dose. AKT inhibition was also apparent in the ganitumab-treated xenografts with 50% inhibition observed at the 100 and 300 μg doses. No inhibition of INSR was observed (Fig. 5B).

To assess the mechanism of action of ganitumab in OV-90 xenografts, we studied changes in apoptosis and proliferation by measuring caspase-3 expression and BrdUrd incorporation in OV-90 xenografts following a single dose of ganitumab. Immunohistochemical analysis of OV-90 xenografts showed that ganitumab treatment had no effect on caspase-3 expression (data not shown) but decreased BrdUrd incorporation at 24 hours post-dose (Fig. 5C).

Growth inhibition of TOV-21G xenografts by ganitumab was completely absent at any dose (Fig. 5D). Consistent with the *in vitro* results, analysis of IGF-IR, INSR, and AKT activation at the end of the xenograft study showed no effect (Fig. 5E).

Effects of ganitumab with chemotherapy *in vitro* and *in vivo*

Multiple drug effect analyses were performed to determine the nature of interactions between ganitumab and the platinum salts carboplatin or paclitaxel, which are commonly used for the treatment of primary and recurrent ovarian cancer. The cell lines that were most responsive to ganitumab in anchorage-dependent assays (KK and OVCAR-5 cells) and in anchorage-independent assays (OV-90 and OVCAR-3 cells) were examined. Synergistic interactions were observed when ganitumab was combined with carboplatin in 3 of the 4 cell lines examined {mean combination index values ranged between 0.39 [95% confidence interval (CI), 0.24–0.54, $P < 0.001$] in OVCAR-5 cells and 1.01 [95% CI, 0.85–1.18, $P = 0.862$] in OVCAR-3 cells; Fig. 6A]. Synergistic interactions were also observed when ganitumab was combined with paclitaxel in 3 of the 4 cell lines examined [mean combination index values ranged between 0.41 (95% CI, 0.29–0.52, $P < 0.001$) in OVCAR-5 cells and 0.67 (95% CI, 0.15–1.19, $P = 0.175$) in OVCAR-3 cells; Fig. 6A].

The efficacy of ganitumab in combination with the platinum salt cisplatin was further tested against established OV-90 and OVCAR-3 xenografts (Fig. 6B and C). Cisplatin alone (4 mg/kg: OV-90 and 2.5 mg/kg: OVCAR-3) significantly inhibited tumor growth in both models. The OVCAR-3 model displayed higher sensitivity to cisplatin treatment with a 2.5 mg/kg dose, twice per week, achieving better than 90% tumor growth inhibition. In the OV-90 model, a 4 mg/kg dose of cisplatin was necessary to achieve 60% tumor growth inhibition.

In contrast, the OVCAR-3 model was more resistant to the effects of ganitumab as a single agent with the 300 μg/dose producing only 50% tumor growth inhibition, when only a 30

μg/dose was necessary in the OV-90 model to achieve the same tumor growth inhibition effect. Combination treatment in both models produced potent tumor growth inhibition effects leading to cytostasis in the OV-90 model and tumor regression in the OVCAR-3 model. Analysis by RMANOVA confirmed that the efficacy achieved by the combination of ganitumab and cisplatin was significantly better than the efficacy achieved with either agent alone in the OV-90 ($P < 0.001$) and OVCAR-3 xenograft model ($P < 0.001$; Fig. 6B and C).

Discussion

Activation of the PI3K/AKT signaling pathway, leading to tumor cell survival and drug resistance, has been shown to be common in human cancers (25). In ovarian cancer, activation of this pathway occurs through activating PI3K mutations, PI3K overexpression, AKT2 amplification, PTEN loss, and IGF-II overexpression (14, 26–28). These genotypic changes lead to tumor cell proliferation, decreased apoptosis, and resistance to chemotherapy (29). Agents able to reverse activation of the PI3K/AKT pathway represent a promising new treatment strategy for ovarian cancer. Here, we have evaluated the ability of ganitumab to reverse PI3K/AKT pathway activation and inhibit tumor growth. Our findings suggest that ganitumab may be effective against ovarian cancer cells in which the PI3K/AKT pathway has been activated by increased IGF-II expression and IGF-IR signaling. In contrast, ovarian cancer cells in which activation of the PI3K/AKT pathway occurs through deletion of the tumor suppressor gene PTEN and/or increased sensitivity to insulin may be less sensitive to ganitumab. Similar observations have been made in the treatment of colorectal cancer, where oncogenic activation of the EGF receptor (EGFR) downstream effector KRAS can attenuate the efficacy of cetuximab and panitumumab, 2 monoclonal antibodies that target EGFR. Because cetuximab and panitumumab act by blocking ligand-dependent activation of EGFR, these agents are not effective against KRAS-mutant colorectal tumors (30).

Our data indicated a significant correlation between IGF-II expression and sensitivity to ganitumab. OV-90 cells, which express IGF-II when grown in cell culture or as xenografts, showed increased sensitivity to ganitumab. This degree of sensitivity, which is comparable to that observed in SJSA-1 xenografts (also an IGF-II–expressing model; ref. 31), is also likely driven by an IGF-IR/IGF-II autocrine loop. The ability of ganitumab to block IGF-II–dependent AKT activation in the OV-90 cell line supports this hypothesis as activation of AKT by IGF-II through INSR homodimers would otherwise render ganitumab less effective against IGF-II treatment (19). Even though IGF-I expression did not significantly correlate with sensitivity to ganitumab, a strong trend toward significance was observed in both anchorage-dependent ($P = 0.081$) and anchorage-independent ($P = 0.119$) data sets. In addition, the OVCAR-3 model displayed relative high IGF-I expression and was sensitive to ganitumab. In an effort to further understand IGF-I and IGF-II expression in high-grade serous ovarian cancers, we looked at 489 cases available in the TCGA database (12) and another 174 cases from a Mayo Clinic cohort (Konecny and colleagues, manuscript in preparation). The analysis showed that IGF-I was significantly higher in the mesenchymal subtype, whereas IGF-II was higher in the differentiated molecular subtype. We hypothesize that both of these subtypes, representing about 20% of high-grade serous cancers each, may preferentially benefit from therapeutic interdiction of the IGF-IR signaling pathway.

Consistent with other PTEN-null cell lines, we were able to detect high basal levels of phospho-AKT in TOV-21G cells (32, 33). The inability of ganitumab to inhibit pAKT in TOV-21G cells suggests that AKT signaling is IGF-IR/hybrid receptor independent. Our signaling data, furthermore, showed that TOV-21G cells were most responsive to insulin stimulation, but this signaling activity was completely refractory to inhibition by ganitumab. Therefore, PI3K/AKT pathway activation in TOV-21G cells may depend on both insulin stimulation and low expression of PTEN. Both attributes were associated with resistance to ganitumab and may thus represent clinically useful exclusion criteria for anti–IGF-IR therapy. Earlier reports suggest that increased expression of insulin and its receptor, especially of the splice variant A, may be important predictors of resistance to IGF-IR inhibitors (8, 34). Development of assays that would allow assessment and quantification of IGF-IR and INSR receptor hybrids may enhance our ability to predict response to ganitumab and other anti–IGF-IR antibodies (8). Moreover, with the emergence of high-throughput molecular techniques, distinct molecular signatures have been identified in ovarian cancer that may also aid in the future selection of patients that likely benefit from IGF-IR inhibition (35, 36).

Platinum- and taxane-based chemotherapy has improved clinical outcomes in patients diagnosed with ovarian cancer. However, primary or secondary resistance to these agents is common (2, 3). The PI3K/AKT signaling pathway has been implicated in the development of resistance to both platinum salts and taxanes (37). Preclinical studies have demonstrated an activation of AKT signaling following treatment with paclitaxel or cisplatin (38). Conversely, inhibition of AKT leads to increased cell death in ovarian cancer cells treated with paclitaxel or cisplatin (39). Other preclinical studies have similarly shown that increased activity of IGF-IR or increased expression of IGF-II was associated with resistance to paclitaxel or cisplatin in ovarian cancer models (18, 40). Consistent with these observations, our *in vitro* and *in vivo* findings indicate that ganitumab was able to significantly increase the activity of carboplatin/cisplatin or paclitaxel in ganitumab-sensitive ovarian cancer cell lines.

In summary, our preclinical evaluation of ganitumab in ovarian carcinoma models suggests that inhibition of IGF-IR may be beneficial for a specific subset of patients diagnosed with ovarian cancer. Tumors that are driven by IGF-II signaling through IGF-IR or hybrid receptor signaling may be particularly sensitive to ganitumab. On the other hand, tumors that display PTEN deletions and/or hypersensitivity to insulin holoreceptor signaling may likely show resistance to ganitumab. Taken together, our findings support further clinical evaluation of ganitumab as a single agent or in combination with chemotherapy in patients with ovarian cancer. Most importantly, the assessment of functionally implicated response predictors in these clinical trials may help to identify the patient subgroup most likely to benefit from treatment with ganitumab.

Supplementary Material

Refer to Web version on PubMed Central for supplementary material.

Acknowledgments

The authors thank Grace Chung and Larry Daugherty for assistance with flow cytometry; Efrain Pacheco for assistance with immunohistochemistry; Pani Kiaei and Mike Damore for assistance with qRT-PCR; and Kerri Hebard-Massey for editorial assistance.

Grant Support

This work has been supported in part by the Dr Miriam and Sheldon G. Adelson Medical Research Foundation and funded in part by Amgen Inc.

References

1. Jemal A, Siegel R, Xu J, Ward E. Cancer statistics, 2010. CA Cancer J Clin. 2010; 60:277–300. [PubMed: 20610543]
2. Bookman MA, Brady MF, McGuire WP, Harper PG, Alberts DS, Friedlander M, et al. Evaluation of new platinum-based treatment regimens in advanced-stage ovarian cancer: a Phase III Trial of the Gynecologic Cancer Intergroup. J Clin Oncol. 2009; 27:1419–1425. [PubMed: 19224846]
3. Katsumata N, Yasuda M, Takahashi F, Isonishi S, Jobo T, Aoki D, et al. Dose-dense paclitaxel once a week in combination with carboplatin every 3 weeks for advanced ovarian cancer: a phase 3, open-label, randomised controlled trial. Lancet. 2009; 374:1331–1338. [PubMed: 19767092]
4. Bruchim I, Werner H. Targeting IGF-1 signaling pathways in gynecologic malignancies. Expert Opin Ther Targets. 2013; 17:307–320. [PubMed: 23294364]
5. Pollak MN, Schernhammer ES, Hankinson SE. Insulin-like growth factors and neoplasia. Nat Rev Cancer. 2004; 4:505–518. [PubMed: 15229476]
6. Frasca F, Pandini G, Scalia P, Sciacca L, Mineo R, Costantino A, et al. Insulin receptor isoform A, a newly recognized, high-affinity insulin-like growth factor II receptor in fetal and cancer cells. Mol Cell Biol. 1999; 19:3278–3288. [PubMed: 10207053]
7. Tobin G, Yee D, Brunner N, Rotwein P. A novel human insulin-like growth factor I messenger RNA is expressed in normal and tumor cells. Mol Endocrinol. 1990; 4:1914–1920. [PubMed: 2082190]
8. Yee D. Insulin-like growth factor receptor inhibitors: baby or the bathwater? J Natl Cancer Inst. 2012; 104:975–981. [PubMed: 22761272]
9. Kwintkiewicz J, Giudice LC. The interplay of insulin-like growth factors, gonadotropins, and endocrine disruptors in ovarian follicular development and function. Semin Reprod Med. 2009; 27:43–51. [PubMed: 19197804]
10. Lucy MC. Growth hormone regulation of follicular growth. Reprod Fertil Dev. 2011; 24:19–28. [PubMed: 22394714]
11. An Y, Cai L, Wang Y, Zhu D, Guan Y, Zheng J. Local expression of insulin-like growth factor-I, insulin-like growth factor-I receptor, and estrogen receptor alpha in ovarian cancer. Onkologie. 2009; 32:638–644. [PubMed: 19887867]
12. National Cancer Institute. [cited 2014 Feb] The Cancer Genome Atlas. Available from: http://cancergenome.nih.gov/
13. Lu L, Katsaros D, Wiley A, Rigault de la Longrais IA, Risch HA, Puopolo M, et al. The relationship of insulin-like growth factor-II, insulin-like growth factor binding protein-3, and estrogen receptor-alpha expression to disease progression in epithelial ovarian cancer. Clin Cancer Res. 2006; 12:1208–1214. [PubMed: 16489075]
14. Sayer RA, Lancaster JM, Pittman J, Gray J, Whitaker R, Marks JR, et al. High insulin-like growth factor-2 (IGF-2) gene expression is an independent predictor of poor survival for patients with advanced stage serous epithelial ovarian cancer. Gynecol Oncol. 2005; 96:355–361. [PubMed: 15661221]
15. Pearce CL, Doherty JA, Van Den Berg DJ, Moysich K, Hsu C, Cushing-Haugen KL, et al. Genetic variation in insulin-like growth factor 2 may play a role in ovarian cancer risk. Hum Mol Genet. 2011; 20:2263–2272. [PubMed: 21422097]

16. Murphy SK, Huang Z, Wen Y, Spillman MA, Whitaker RS, Simel LR, et al. Frequent IGF2/H19 domain epigenetic alterations and elevated IGF2 expression in epithelial ovarian cancer. Mol Cancer Res. 2006; 4:283–292. [PubMed: 16603642]

17. Rainier S, Johnson LA, Dobry CJ, Ping AJ, Grundy PE, Feinberg AP. Relaxation of imprinted genes in human cancer. Nature. 1993; 362:747–749. [PubMed: 8385745]

18. Huang GS, Brouwer-Visser J, Ramirez MJ, Kim CH, Hebert TM, Lin J, et al. Insulin-like growth factor 2 expression modulates Taxol resistance and is a candidate biomarker for reduced disease-free survival in ovarian cancer. Clin Cancer Res. 2010; 16:2999–3010. [PubMed: 20404007]

19. Beltran PJ, Mitchell P, Chung YA, Cajulis E, Lu J, Belmontes B, et al. AMG 479, a fully human anti-insulin-like growth factor receptor type I monoclonal antibody, inhibits the growth and survival of pancreatic carcinoma cells. Mol Cancer Ther. 2009; 8:1095–1105. [PubMed: 19366899]

20. Konecny GE, Winterhoff B, Kolarova T, Qi J, Manivong K, Dering J, et al. Expression of p16 and retinoblastoma determines response to CDK4/6 inhibition in ovarian cancer. Clin Cancer Res. 2011; 17:1591–1602. [PubMed: 21278246]

21. Sjoblom T, Jones S, Wood LD, Parsons DW, Lin J, Barber TD, et al. The consensus coding sequences of human breast and colorectal cancers. Science. 2006; 314:268–274. [PubMed: 16959974]

22. Gowan SM, Hardcastle A, Hallsworth AE, Valenti MR, Hunter LJ, de Haven Brandon AK, et al. Application of meso scale technology for the measurement of phosphoproteins in human tumor xenografts. Assay Drug Dev Technol. 2007; 5:391–401. [PubMed: 17638539]

23. Pegram MD, Konecny GE, O'Callaghan C, Beryt M, Pietras R, Slamon DJ. Rational combinations of trastuzumab with chemotherapeutic drugs used in the treatment of breast cancer. J Natl Cancer Inst. 2004; 96:739–749. [PubMed: 15150302]

24. Polverino A, Coxon A, Starnes C, Diaz Z, DeMelfi T, Wang L, et al. AMG 706, an oral, multikinase inhibitor that selectively targets vascular endothelial growth factor, platelet-derived growth factor, and kit receptors, potently inhibits angiogenesis and induces regression in tumor xenografts. Cancer Res. 2006; 66:8715–8721. [PubMed: 16951187]

25. Engelman JA, Luo J, Cantley LC. The evolution of phosphatidylinositol 3-kinases as regulators of growth and metabolism. Nat Rev Genet. 2006; 7:606–619. [PubMed: 16847462]

26. Cheng JQ, Godwin AK, Bellacosa A, Taguchi T, Franke TF, Hamilton TC, et al. AKT2, a putative oncogene encoding a member of a subfamily of protein-serine/threonine kinases, is amplified in human ovarian carcinomas. Proc Natl Acad Sci U S A. 1992; 89:9267–9271. [PubMed: 1409633]

27. Lin WM, Forgacs E, Warshal DP, Yeh IT, Martin JS, Ashfaq R, et al. Loss of heterozygosity and mutational analysis of the PTEN/MMAC1 gene in synchronous endometrial and ovarian carcinomas. Clin Cancer Res. 1998; 4:2577–2583. [PubMed: 9829719]

28. Shayesteh L, Lu Y, Kuo WL, Baldocchi R, Godfrey T, Collins C, et al. PIK3CA is implicated as an oncogene in ovarian cancer. Nat Genet. 1999; 21:99–102. [PubMed: 9916799]

29. Carden CP, Stewart A, Thavasu P, Kipps E, Pope L, Crespo M, et al. The association of PI3 kinase signaling and chemoresistance in advanced ovarian cancer. Mol Cancer Ther. 2012; 11:1609–1617. [PubMed: 22556379]

30. Amado RG, Wolf M, Peeters M, Van Cutsem E, Siena S, Freeman DJ, et al. Wild-type KRAS is required for panitumumab efficacy in patients with metastatic colorectal cancer. J Clin Oncol. 2008; 26:1626–1634. [PubMed: 18316791]

31. Beltran PJ, Chung YA, Moody G, Mitchell P, Cajulis E, Vonderfecht S, et al. Efficacy of ganitumab (AMG 479), alone and in combination with rapamycin, in Ewing's and osteogenic sarcoma models. J Pharmacol Exp Ther. 2011; 337:644–654. [PubMed: 21385891]

32. Colakoglu T, Yildirim S, Kayaselcuk F, Nursal TZ, Ezer A, Noyan T, et al. Clinicopathological significance of PTEN loss and the phosphoinositide 3-kinase/Akt pathway in sporadic colorectal neoplasms: is PTEN loss predictor of local recurrence? Am J Surg. 2008; 195:719–725. [PubMed: 18440486]

33. Vitolo MI, Weiss MB, Szmacinski M, Tahir K, Waldman T, Park BH, et al. Deletion of PTEN promotes tumorigenic signaling, resistance to anoikis, and altered response to chemotherapeutic

agents in human mammary epithelial cells. Cancer Res. 2009; 69:8275–8283. [PubMed: 19843859]

34. Buck E, Gokhale PC, Koujak S, Brown E, Eyzaguirre A, Tao N, et al. Compensatory insulin receptor (IR) activation on inhibition of insulin-like growth factor-1 receptor (IGF-1R): rationale for cotargeting IGF-1R and IR in cancer. Mol Cancer Ther. 2010; 9:2652–2664. [PubMed: 20924128]
35. Attias-Geva Z, Bentov I, Kidron D, Amichay K, Sarfstein R, Fishman A, et al. p53 Regulates insulin-like growth factor-I receptor gene expression in uterine serous carcinoma and predicts responsiveness to an insulin-like growth factor-I receptor-directed targeted therapy. Eur J Cancer. 2012; 48:1570–1580. [PubMed: 22033326]
36. Kobel M, Kalloger SE, Boyd N, McKinney S, Mehl E, Palmer C, et al. Ovarian carcinoma subtypes are different diseases: implications for biomarker studies. PLoS Med. 2008; 5:e232. [PubMed: 19053170]
37. Westfall SD, Skinner MK. Inhibition of phosphatidylinositol 3-kinase sensitizes ovarian cancer cells to carboplatin and allows adjunct chemotherapy treatment. Mol Cancer Ther. 2005; 4:1764–1771. [PubMed: 16275998]
38. Mabuchi S, Ohmichi M, Kimura A, Hisamoto K, Hayakawa J, Nishio Y, et al. Inhibition of phosphorylation of BAD and Raf-1 by Akt sensitizes human ovarian cancer cells to paclitaxel. J Biol Chem. 2002; 277:33490–33500. [PubMed: 12087097]
39. Hayakawa J, Ohmichi M, Kurachi H, Kanda Y, Hisamoto K, Nishio Y, et al. Inhibition of BAD phosphorylation either at serine 112 via extracellular signal-regulated protein kinase cascade or at serine 136 via Akt cascade sensitizes human ovarian cancer cells to cisplatin. Cancer Res. 2000; 60:5988–5994. [PubMed: 11085518]
40. Eckstein N, Servan K, Hildebrandt B, Politz A, von Jonquieres G, Wolf-Kummeth S, et al. Hyperactivation of the insulin-like growth factor receptor I signaling pathway is an essential event for cisplatin resistance of ovarian cancer cells. Cancer Res. 2009; 69:2996–3003. [PubMed: 19318572]

Translational Relevance

The insulin-like growth factor 1 receptor (IGF-IR) pathway is an important regulator of tumor biology that has been implicated in the pathogenesis of ovarian cancer. Ganitumab is an investigational, fully human monoclonal antibody against IGF-IR that blocks binding of both endogenous IGF-IR ligands IGF-I and IGF-II. Here, we evaluate the ability of ganitumab to reverse phosphoinositide 3-kinase (PI3K)/AKT pathway activation and inhibit tumor growth. Our findings suggest that ganitumab may be beneficial against ovarian cancer cells that use IGF-II expression in conjunction with IGF-IR activity to activate the PI3K/AKT pathway. In contrast, ovarian cancer cells in which activation of the PI3K/AKT pathway occurs through deletion of the tumor suppressor gene PTEN and/or increased sensitivity to insulin will likely be resistant to ganitumab.

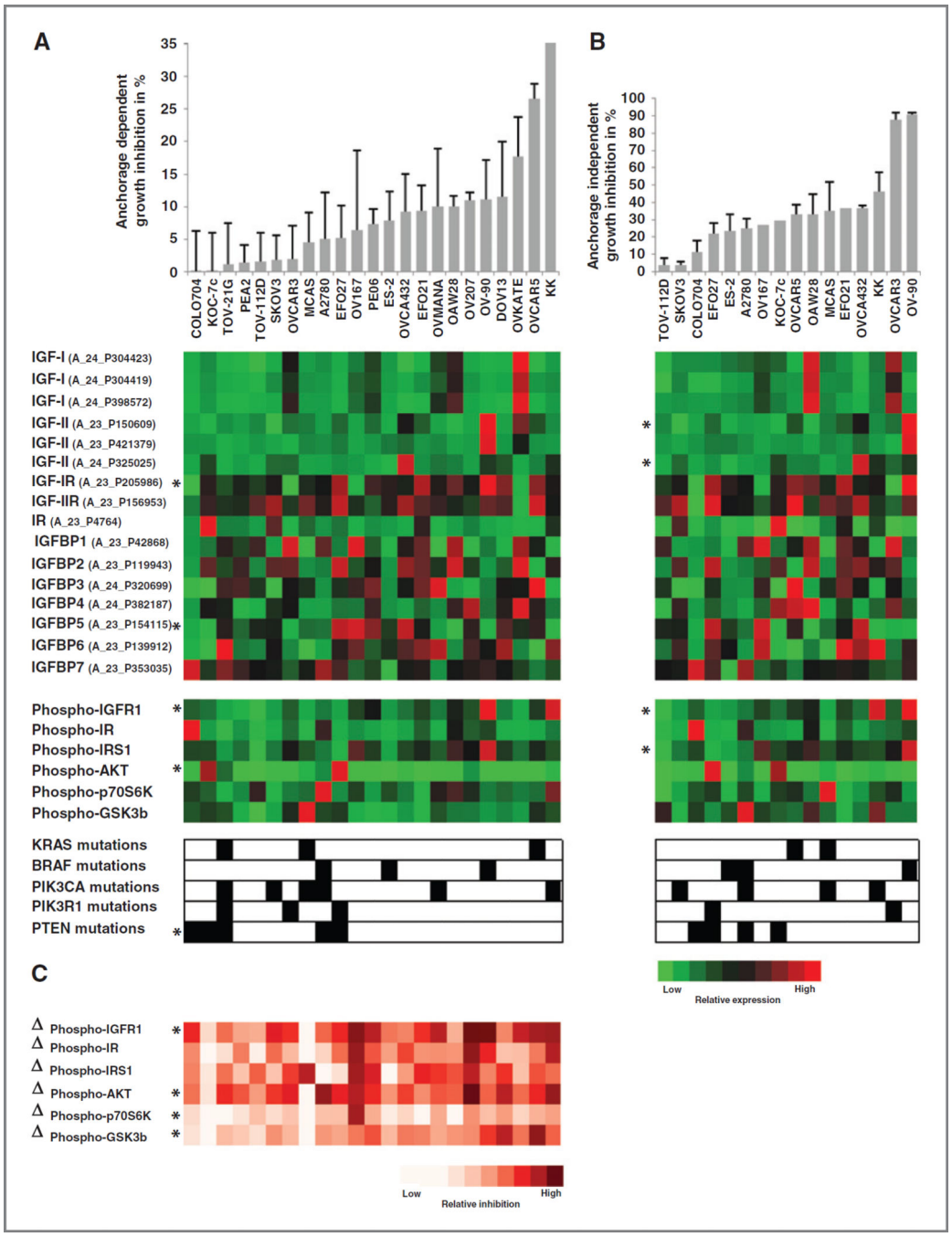

Figure 1.

The effects of ganitumab on human ovarian cancer cells were evaluated using a panel of 23 established human ovarian cancer cell lines. Cells were treated with 100 μg/mL (0.68 μmol/L) ganitumab, and anchorage-dependent and anchorage-independent growth inhibition was assessed using 2-dimensional (2D) assays (A) and 3D soft agar assays (B), respectively. Cell lines are ordered from low growth inhibition values to high growth inhibition values. C, the IGF/IGF-IR signaling pathway was characterized in each of the 23 ovarian cancer cell lines using the Agilent Human 44K gene expression profiling array chip, a Mesoscale

multiplexed ELISA assay which measures total and phosphorylated proteins, and sequencing of the *PIK3CA, PIK3R1, PTEN, KRAS*, and *BRAF* genes. Each of these markers was assessed at baseline. The red and green matrices represent the expression patterns for each gene. Brightest red indicates highest relative expression; brightest green indicates lowest relative expression. A black square indicates the presence of a mutation and a white square the absence of a mutation. In addition, we assessed the percentage of inhibition of phosphorylation following 1-hour treatment with 100 μg/mL (0.68 μmol/L) ganitumab compared with baseline levels, which is depicted as Δphospho-proteins. The red and white matrices represent the differential expression patterns for each phosphorylated protein. Brightest red indicates highest inhibition of phosphorylation. *, significant correlations between growth inhibition and biomarkers.

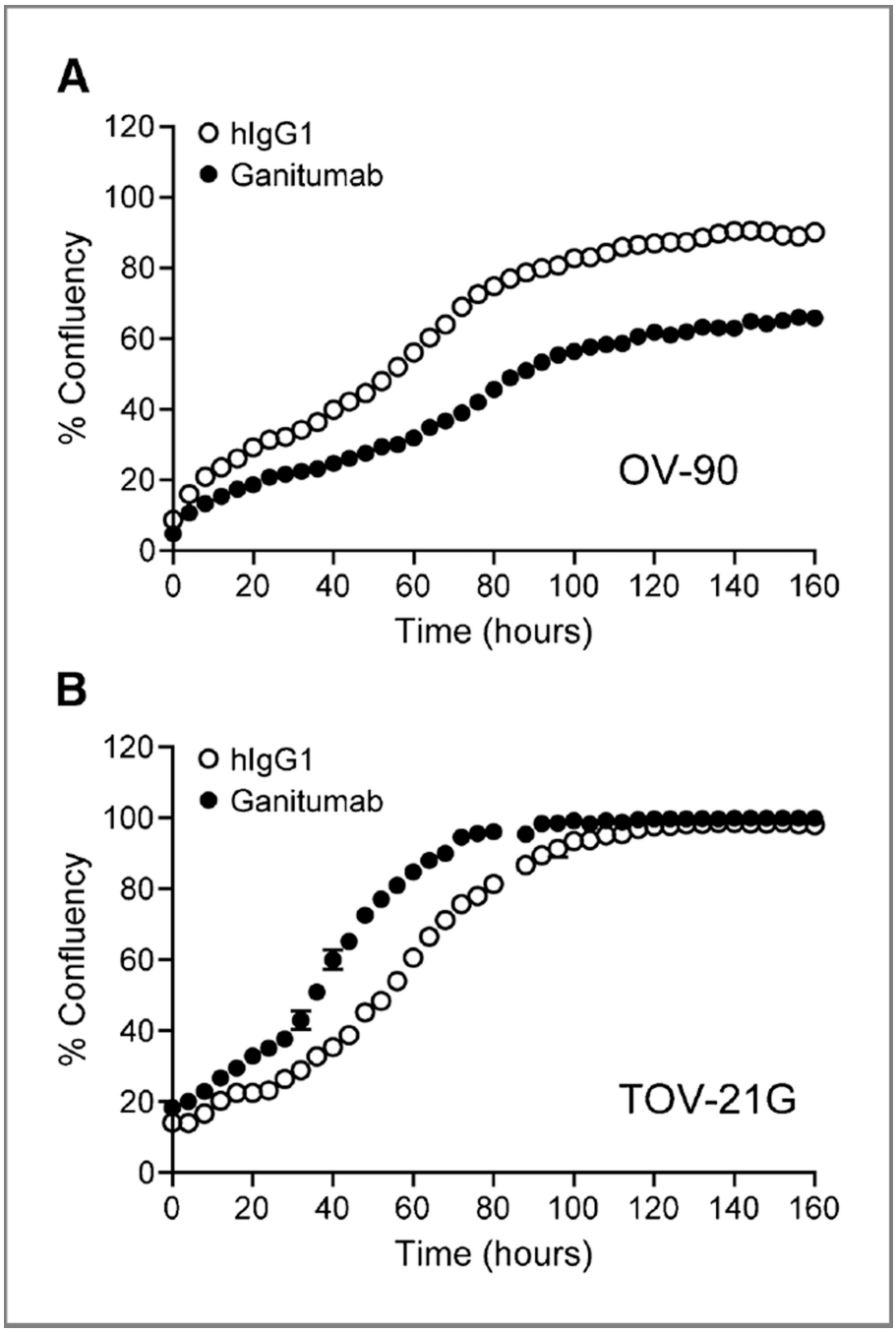

Figure 2.

The effect of ganitumab on cell growth *in vitro*. The growth of OV-90 (A) and TOV-21G cells (B) in complete culture media was measured using IncuCyte technology, which monitored cell confluency at 4-hour intervals. The percentage confluency was plotted versus time in the presence of control hIgG1 or ganitumab.

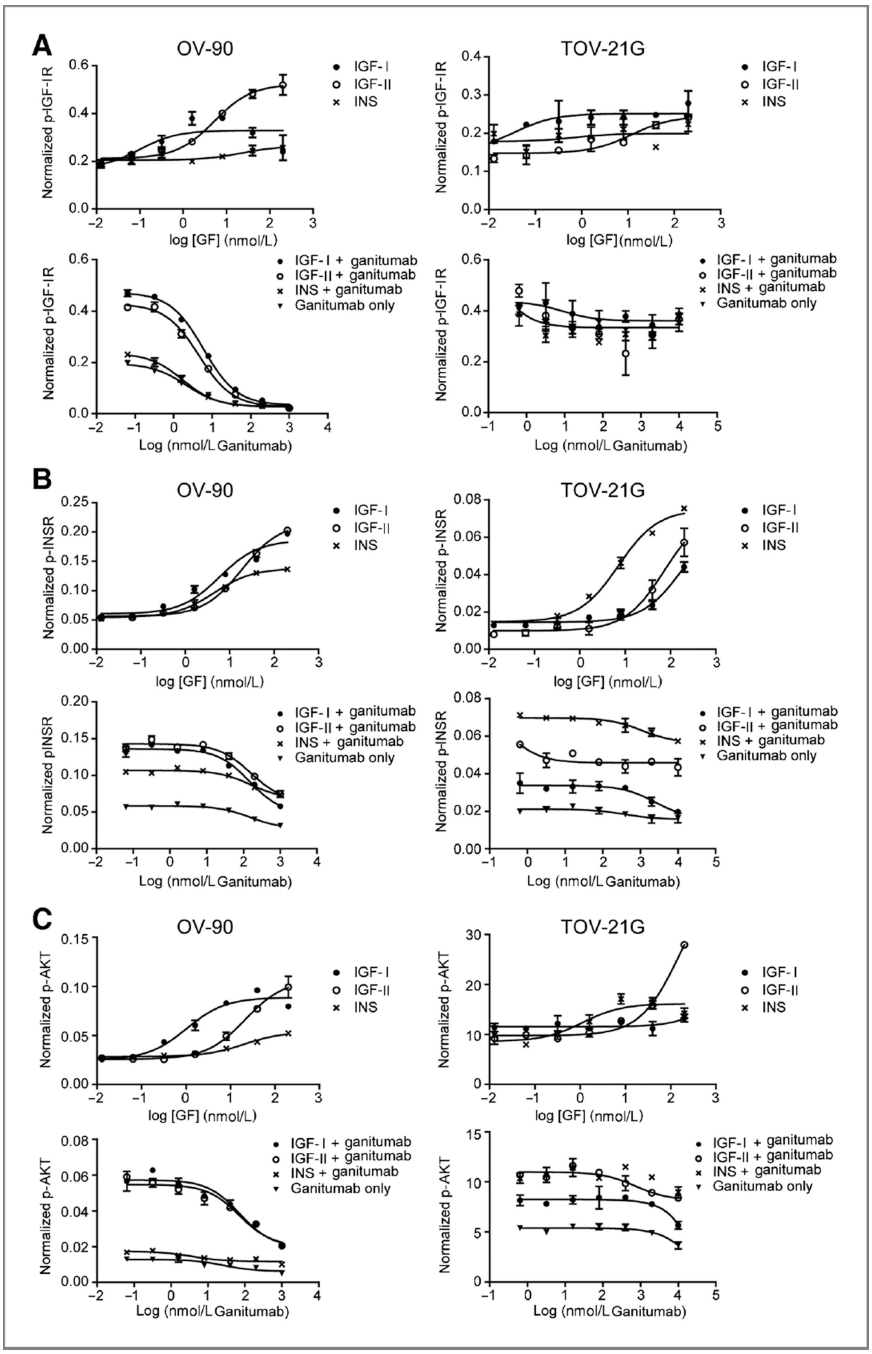

Figure 3.

Induction and blockade of growth factor–induced IGF-IR, INSR, and AKT signaling with IGF-II, IGF-II, insulin, and ganitumab. A, ganitumab inhibited IGF-I–, IGF-II–, and insulin-induced IGF-IR phosphorylation in OV-90 cells but not in TOV-21G cells. B, ganitumab inhibited IGF-I–, IGF-II–, and insulin-induced INSR phosphorylation in OV-90 cells. Only IGF-I–induced INSR phosphorylation was inhibited in the TOV-21G cell line. C, ganitumab inhibited IGF-I– and IGF-II–induced AKT phosphorylation in OV-90 cells but not in TOV-21G cells. Phosphorylated and total IGF-IR, INSR, and AKT levels were determined

in serum-starved OV-90 and TOV-21G cells after 20 minutes of treatment with growth factor ± ganitumab using Mesoscale multiplex assays. Mean data are plotted as phosphoprotein signal divided by total signal without background subtraction ± SD.

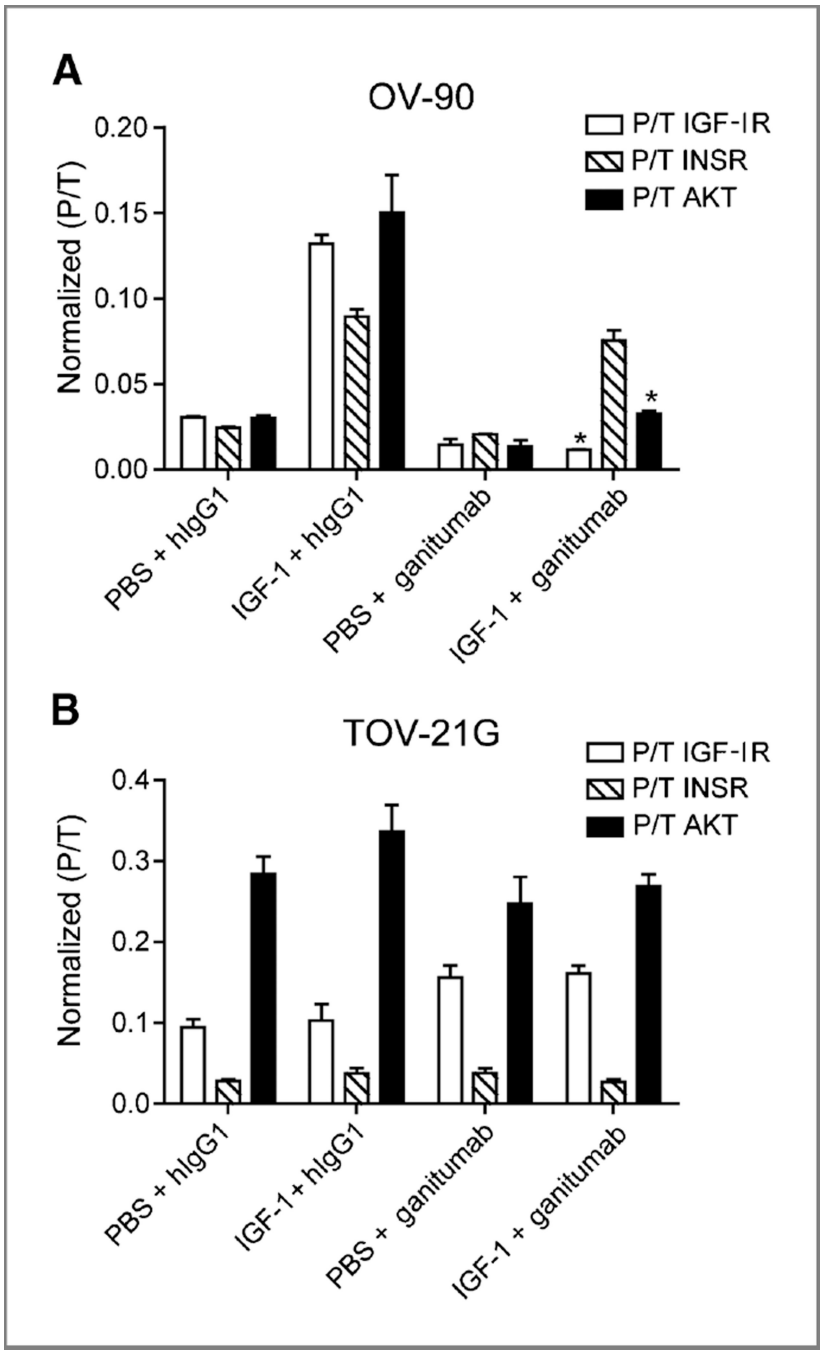

Figure 4.

Blockade of IGF-I–induced IGF-IR and hybrid receptor signaling in human ovarian cancer xenografts by ganitumab. Mice bearing OV-90 or TOV-21G xenografts between 300 and 450 mm^3 (*n*= 3 per group) were injected intraperitoneally with 1 mg ganitumab or hIgG1. After 6 hours, IGF-I (5 μg) or 1× PBS was administered intravenously, and after 15 minutes, xenografts were collected and analyzed for levels of phosphorylated IGF-IR, INSR, and AKT. A, ganitumab inhibited IGF-IR and AKT but not INSR phosphorylation in OV-90 xenografts. B, ganitumab did not inhibit IGF-IR, INSR, and AKT phosphorylation in

TOV-21G xenografts. Data, mean ± SEM. Student *t* test was used to determine whether ganitumab significantly nhibited the activation of IGF-IR, INSR, or AKT when compared with hIgG1 control. *, $P < 0.01$.

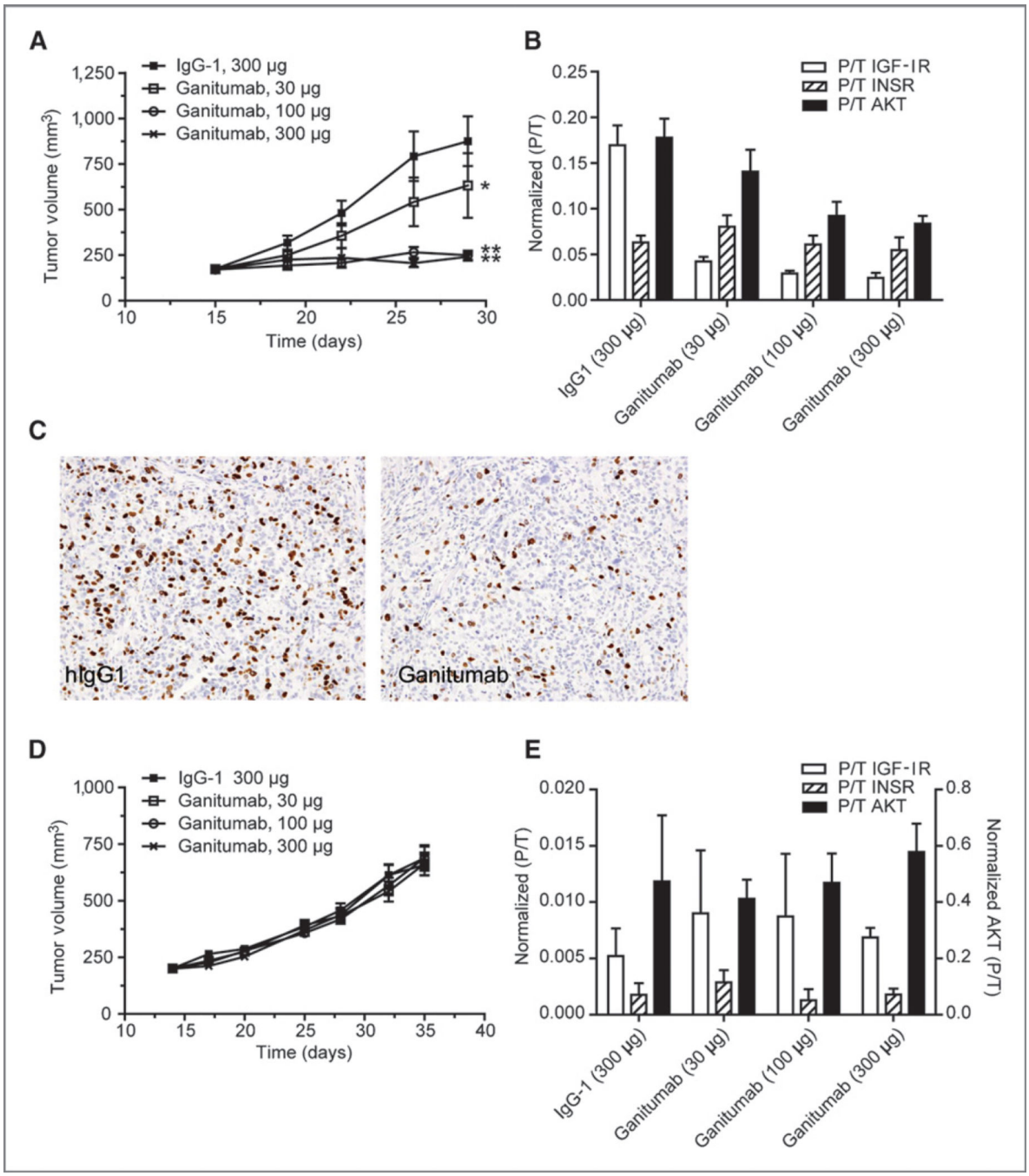

Figure 5.

Efficacy of ganitumab in ovarian cancer models. Mice bearing about 200 mm^3 OV-90 or TOV-21G xenografts were randomly assigned into 4 treatment groups and treated intraperitoneally twice per week with ganitumab (30, 100, or 300 µg/dose) or hIgG1 (300 µg/dose). Tumor volumes were measured twice per week using calipers. Data, mean volume ± SEM. A, ganitumab significantly inhibited OV-90 tumor growth (*, P= 0.041; ** ,P= 0.0001 vs. control hIgG1 group). B, level of phosphorylated/total IGF-IR, INSR, and AKT in OV-90 xenografts at the end of the efficacy study. OV-90 xenografts were collected 6

hours after the last dose of ganitumab (*n*= 2 per time point per group). Total and phosphorylated receptor levels were measured using MSD multiplex assay. Data, mean ± SD. C, inhibition of OV-90 cell proliferation by ganitumab. Mice bearing OV-90 xenografts (~300 mm^3) were treated with 1 mg of ganitumab or hIgG1 for 24 hours. Xenografts were harvested, fixed in zinc formalin, embedded in paraffin, and processed for BrdUrd detection by immunohistochemistry. Photomicrographs were taken at 200x magnification. D, ganitumab did not inhibit TOV-21G tumor growth. E, ganitumab did not inhibit IGF-IR signaling in TOV-21G xenografts.

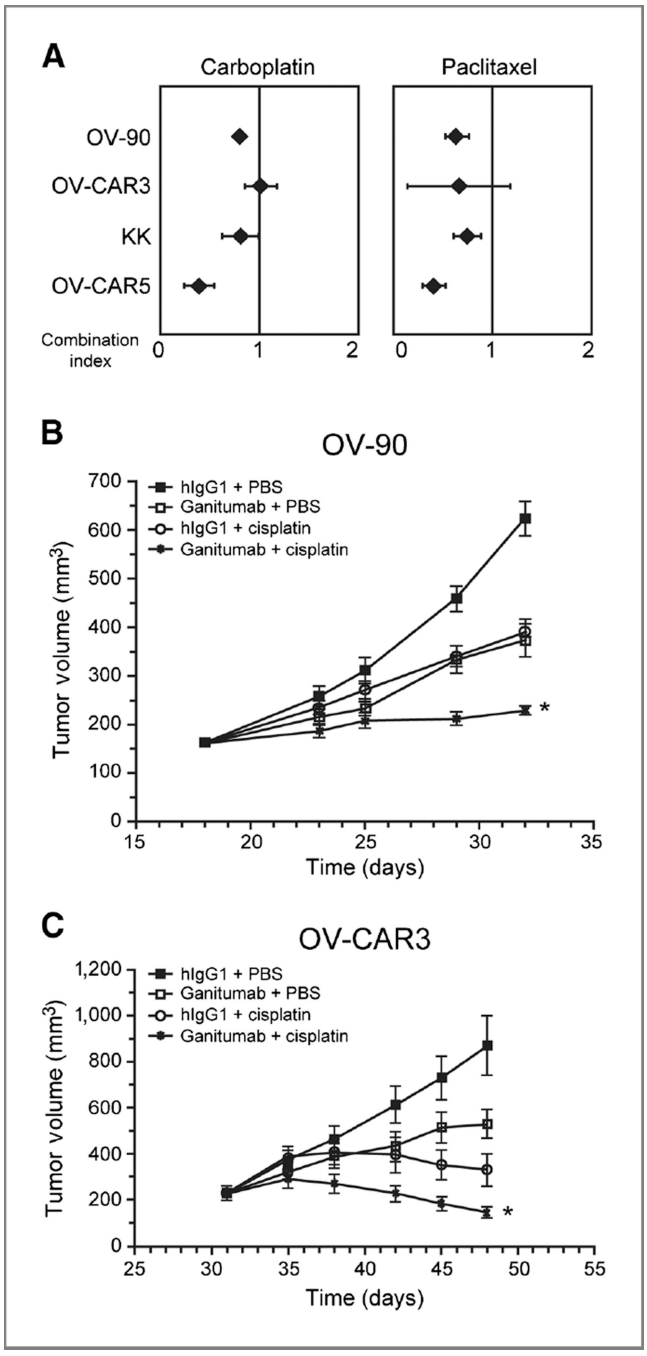

Figure 6.

Efficacy of ganitumab in combination with chemotherapeutic agents. A, multiple drug effect analyses were performed to determine the nature of interactions between ganitumab and chemotherapeutic agents commonly used for the treatment of primary and recurrent ovarian cancer. Combination index values were derived from variables of the median effect plots, and statistical tests were applied to determine whether the mean combination values at multiple effect levels (IC_{20}–IC_{80}) were significantly different from 1.0. In this analysis, synergy was defined as combination index values significantly lower than 1.0, antagonism

as combination index values significantly higher than 1.0, and additivity as combination index values equal to 1.0. B, mice bearing about 200 mm^3 OV-90 or (C) OVCAR-3 xenografts were randomly assigned into 4 treatment groups and treated intraperitoneally twice per week with ganitumab (300 μg/dose), hIgG1 (300 μg/dose), cisplatin (2.5 or 4.0 mg/kg), or a combination of ganitumab plus cisplatin: (OV-90, 30 μg/dose + 4.0 mg/kg; OV-CAR-3, 300 μg/dose + 2.5 mg/kg). Tumor volumes were measured twice per week using calipers. Data, mean volume ± SEM. B and C, ganitumab significantly enhanced the efficacy of cisplatin in the OV-90 (*, $P < 0.001$, 30 mg/dose ganitumab + 4.0 mg/kg cisplatin) and OVCAR-3 (*, $P < 0.001$, 300 mg/dose ganitumab + 2.5 mg/ kg cisplatin) tumor models.